Deuterium Kinetic Isotope Effects and the Mechanism of the Bacterial Luciferase Reaction†

Wilson A. Francisco,‡ Husam M. Abu-Soud,§ Albert J. DelMonte, Daniel A. Singleton,* Thomas O. Baldwin,* and Frank M. Raushel*

Departments of Chemistry and of Biochemistry & Biophysics, Texas A&M University, College Station, Texas 77843

Received September 11, 1997; Revised Manuscript Received December 10, 1997

ABSTRACT: A combined experimental and theoretical investigation of the deuterium isotope effects on the bacterial luciferase reaction is described. The experimental studies focus on determining if the unusual aldehydic deuterium isotope effect of ∼1.5 observed in these reactions is an intrinsic isotope effect resulting from a single rate-limiting step or is a composite of multiple rate-limiting steps. The isotope effect observed is not significantly affected by variation in the aldehyde chain length, changes in the pH over a range of 6−9, use of αC106A and αC106S site-directed mutants, or chloride substitution at the 8-position of the reduced flavin, though the isotope effect is decreased when the 8-methoxy-substituted flavin is used as a substrate. From these observations it is concluded that the aldehydic isotope effect arises from the change in rate of a single kinetic step. A stopped-flow kinetic analysis of the microscopic rate constants for the reactions of 1-[^{1}H]decanal and 1-[^{2}H]decanal in the bacterial luciferase reaction was carried out, and aldehyde hydration isotope effects were determined. From the results it is estimated that the aldehydic deuterium isotope effect is ∼1.9 after formation of an intermediate flavin C4a-hydroperoxy hemiacetal. Ab initio calculations were used to examine the transformation of the aldehyde into a carboxylic acid and to predict isotope effects for possible mechanisms. These calculations indicate that the mechanism involving rate-limiting electron transfer from the flavin C4a-hydroxide to an intermediate dioxirane is consistent with the enigmatic aldehydic isotope effect and that the intermediacy of a dioxirane is energetically plausible.

Bacterial luciferase catalyzes the production of visible light from the reaction of $FMNH_2$,[1] molecular oxygen, and a long-chain aliphatic aldehyde. The first step of the chemical transformation is the formation of a C4a-flavin hydroperoxide (FMNOOH) from the reaction of $FMNH_2$ and molecular oxygen (*1*). The FMNOOH is a stable intermediate in the presence of enzyme and the complex can be isolated using low-temperature chromatography (*2*). In the absence of aldehyde, the intermediate slowly decomposes to FMN and H_2O_2 with little or no emission of visible light (*3*). In the presence of aldehyde, the hydroperoxide is thought to form a C4a-flavin hydroperoxy hemiacetal (FMNOOR) (*4*), although this intermediate has yet to be isolated and structurally characterized. The subsequent decomposition of the hydroperoxy hemiacetal adduct generates an excited-state intermediate which emits a photon of light in the blue region of the spectrum; there is concomitant formation of the carboxylic acid corresponding to the original aldehyde. The ultimate excited-state molecule is thought to be the C4a-flavin hydroxide (FMNOH) (*5*). The eventual dehydration of the FMNOH affords the final product, FMN. These general aspects of the reaction pathway are summarized in Figure 1. However, the fundamental mechanistic details for the generation of the excited-state flavin from the hydroperoxyflavin intermediate and for the formation of the carboxylic acid remain to be determined at the molecular level.

The analysis of kinetic isotope effects has proven to be a very useful tool in the elucidation of enzyme-catalyzed reaction mechanisms (*6*) and many attempts to gain insight into the luciferase mechanism have involved isotope effect determinations. In general, deuterium substitution within the aldehyde substrate of luciferase has a rather modest effect of about 1.5 on the decay rate of the emitted light. Presswood and Hastings obtained a deuterium isotope effect of 1.7 for the decay of bioluminescence using 1-[^{2}H]decanal as a substrate (*7*). In an earlier investigation, Shannon et al. reported isotope effects of 1.7, 1.2, and 1.0 for the oxidation of *n*-decanal, *n*-dodecanal, and *n*-tetradecanal, respectively (*8*). More recently, Tu et al. measured a deuterium isotope effect of 1.5 when *n*-decanal was utilized as the substrate (*9*). Macheroux et al. found values of 1.4 and 1.5 for the oxidation of *n*-octanal and *n*-dodecanal, respectively (*4*).

A consistent mechanistic interpretation of these isotope effects has been elusive. The rearrangement of the C4a-hydroperoxy hemiacetal intermediate necessarily involves

† This work was supported in part by the NIH (GM 33894 and GM 45617) and NSF Grant CHE-9528196 for computational resources.

* To whom correspondence may be addressed (e-mail: raushel@tamu.edu; singleton@chemvx.tamu.edu; baldwin@bioch.tamu.edu).

‡ National Science Foundation Minority Graduate Fellow (1988−1991).

§ Present address: Department of Immunology, Cleveland Clinic Research Institute, Cleveland, OH.

[1] Abbreviations: $FMNH_2$ and FMN, reduced and oxidized riboflavin 5-phosphate; FMNOOH, flavin C4a-hydroperoxide; FMNOOR, flavin C4a-hydroperoxy hemiacetal; FMNOH, flavin C4a-hydroxide; RCHO, *n*-alkyl aldehyde; Bis-Tris, 2-[bis-(hydroxyethyl)amino]-2-(hydroxymethyl)propane-1,3-diol; TES, *N*-[tris(hydroxymethyl)methyl]-2-aminoethanesulfonic acid; CIEEL, chemically induced electron exchange luminescence.

S0006-2960(97)02266-6 CCC: $15.00
Published on Web 02/06/1998

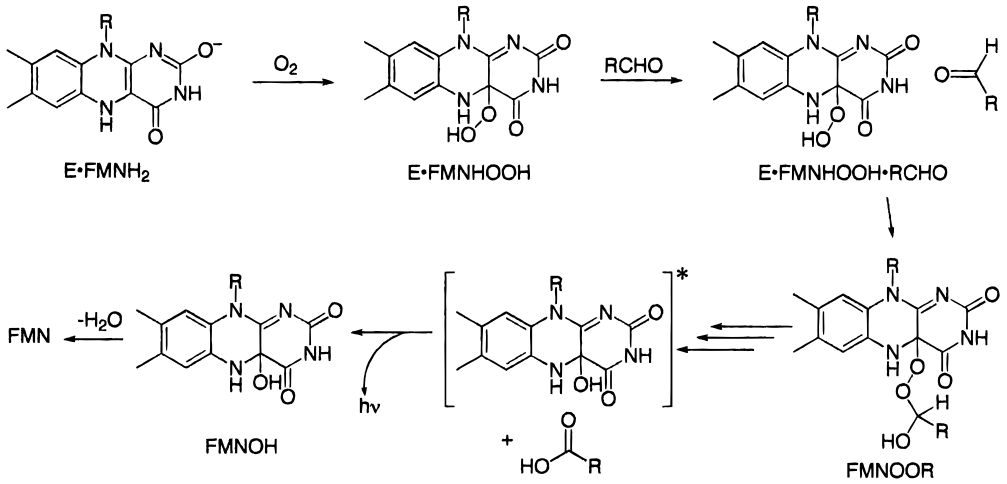

FIGURE 1: Reaction pathway for bacterial-luciferase catalyzed luminescence.

cleavage of the aldehydic proton from the original carbonyl carbon. However, isotope effects of about 1.5 are smaller than the normal range of 2−10 expected for an intrinsic primary isotope effect involving the cleavage of a carbon−hydrogen bond. On the other hand, 1.5 is larger than normally observed for an intrinsic secondary isotope effect. Of course, the observed isotope effect could be a composite of multiple rate-limiting steps, and this is one focus of the current investigation. A second complicating factor is that an inverse secondary deuterium isotope effect is anticipated for the reaction of the C4a-hydroperoxide intermediate with the aldehyde substrate because of the change in hybridization of the central carbon atom from sp^2 to sp^3 upon formation of the putative tetrahedral adduct. This phenomenon has apparently been overlooked in previous investigations. Moreover, a secondary isotope effect by deuterium on the hydration of the aldehyde is also foreseen to play an important factor in the binding of the free aldehyde and/or *gem*-diol to the protein. Finally, the utilization of D_2O solvent is predicted to perturb the proton-transfer steps during substrate turnover.

In this paper, we describe a comprehensive experimental and theoretical investigation of the deuterium isotope effects on the bacterial luciferase reaction. The detailed kinetic mechanism previously constructed (*10, 11*) allows here a determination of the substrate and solvent isotope effects on the individual steps of the kinetic mechanism. At the same time, a series of different aldehyde substrates, flavin derivatives, and mutant enzymes were studied with the idea of modulating the rate-determining step(s) of the reaction and observing the intrinsic isotope effects associated with the individual steps. Finally, ab initio calculations were used to examine the transformation of the aldehyde into a carboxylic acid, and the seemingly enigmatic experimental isotope effects were interpreted with the aid of theoretical isotope effects based on the ab initio calculations. The results provide unique and detailed insight into the molecular mechanism of luciferase bioluminescence.

MATERIALS AND METHODS

General. Riboflavin-5′-monophosphate (FMN) was purchased from Fluka (97%) and used without further purification. Deuterated aldehydes (1-[^{2}H]octanal, 1-[^{2}H]decanal, and 1-[^{2}H]dodecanal) were synthesized from the corresponding 2-[^{2}H]-2-alkyl-1,3-dithianes by cleavage with HgO/HBF_4 in THF (*12*). The 2-[^{2}H]-2-alkyl-1,3-dithianes were prepared from the corresponding 2-[^{1}H]-2-alkyl-1,3-dithianes by deuteration with D_2O (*13*). The 2-[^{1}H]-2-alkyl-1,3-dithianes were prepared by coupling of the corresponding *n*-alkyl aldehydes with 1,3-propanedithiol using BF_3 as a catalyst (*14*). The deuterated aldehydes were characterized by ^{1}H and ^{13}C NMR spectroscopy. Mass spectrometric analysis indicated an isotopic purity of at least 98 atom %. All spectroscopic data were consistent with the expected structures and did not show the presence of any impurities. Unlabeled aldehydes were purchased from Aldrich and distilled under reduced pressure before use. The FMN derivatives were obtained as previously described. All other reagents and solvents were of the highest purity grade available and obtained from either Sigma or Aldrich.

Site-Directed Mutagenesis. Construction of the α106 mutants was performed as described previously (*15*) using a uridinylated single-strand DNA template prepared from *Escherichia coli* strains RZ1032 and CJ236 according to the method of Kunkel et al. (*16*). The mutations were confirmed by dideoxy chain termination sequencing (*17*). A small region of the *lux*A coding region for each mutant was transferred into another plasmid (pLAV11) (*15*) to be certain that the remainder of the coding region had not been altered in the mutagenesis reactions; the sequence of the transferred DNA for each mutant was again determined by dideoxy sequencing.

Enzyme Purification. Wild-type bacterial luciferase from *Vibrio harveyi*, as well as mutant enzymes, was purified by the method of Baldwin et al. (*15*). The enzymes were judged to be greater than 95% pure based on gel electrophoresis. The enzyme concentration was determined spectrophotometrically by measurement of the absorbance at 280 nm using a molecular weight of 76 000 and a specific absorption coefficient of 1.13 cm^{-1} mg^{-1} (*18*).

Stopped-Flow Spectrophotometry. All experiments were performed under a nitrogen atmosphere in 50 mM Bis-Tris-HCl buffer, pH 7.0, at 25 ± 0.2 °C. Care was taken to not expose the flavin solutions to light during the experimental procedures. The flavin was reduced by bubbling hydrogen in the presence of a few crystals of palladium on activated carbon. The concentration of the FMN derivatives was determined spectrophotometrically. The molar absorption

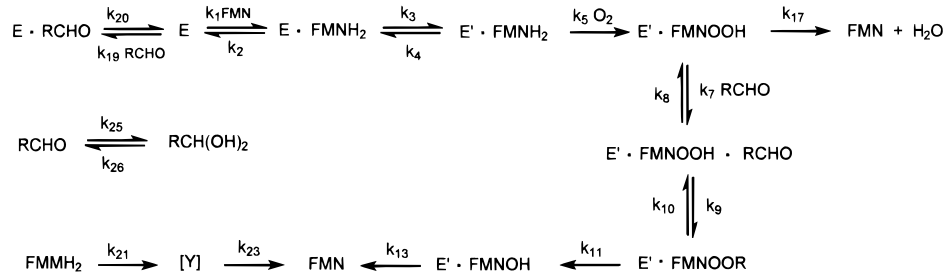

FIGURE 2: Kinetic mechanism for the bacterial luciferase reaction.

coefficients used were 12 200 M^{-1} cm^{-1}at 450 nm for FMN (*19*), 10 100 M^{-1} cm^{-1}at 445 nm for 8-Cl-FMN (*20*), and 24 500 M^{-1} cm^{-1} at 445 nm for 8-CH_3O-FMN (*20*).

The anaerobic enzyme solutions were prepared using an all-glass vacuum system (*21*) by several cycles of evacuation and equilibration with nitrogen gas. Purification of the nitrogen gas was performed by passing the gas over a heated column of BASF catalyst R3-11 (Chemical Dynamics Corp./ Kontes Glass Co.). The anaerobic luciferase-$FMNH_2$ solutions were made by mixing the anaerobic enzyme solutions with reduced flavin under a nitrogen atmosphere, and then the mixture was transferred to the stopped-flow instrument using an airtight Hamilton syringe. The kinetic experiments were carried out using a stopped-flow apparatus from Hi-Tech Ltd. (model SF-51) connected to an HP-300 series computer. The stopped-flow experiments were carried out under the same conditions as described previously (*10, 11*). Stock solutions of 0.1 M aldehyde were freshly prepared before use. The time courses for the various kinetic experiments were fit to one or more of the following rate equations using a nonlinear least-squares procedure contained in the software supplied by Hi-Tech Ltd.

$$y = Ax + C \quad (1)$$

$$y = Ae^{-k_1 t} + C \quad (2)$$

$$y = Ae^{-k_1 t} + Be^{-k_2 t} + C \quad (3)$$

$$y = A[k_1/(k_2 - k_1)](e^{-k_1 t} - e^{-k_2 t}) + C \quad (4)$$

$$y = A[1 + (1/(k_1 - k_2)](k_2 e^{-k_1 t} - k_1 e^{-k_2 t})) + C \quad (5)$$

Equation 3 represents the sum of two independent exponentials for a parallel process and eqs 4 and 5 describe the time courses for a sequential process (X → Y → Z) monitoring the formation of Y and Z, respectively. In these equations, k_1 and k_2 are the first-order rate constants, t is time, and A and B are amplitude factors. Ten individual traces were collected and averaged to improve the signal-to-noise ratio.

All of the kinetic data collected from the stopped-flow studies were transferred to a Silicon Graphics workstation and subsequently analyzed with extensively modified forms of the KINSIM (*22*) and FITSIM (*23*) programs, using the comprehensive kinetic model that appears in Figure 2. The microscopic rate constants that appear in this kinetic model were estimated by comparison of the experimental time courses for product formation with the calculated time courses derived by numerical integration of the appropriate differential equations with the KINSIM program. The rate constants were first estimated graphically until the simulated time courses matched the experimental data as closely as possible. The final values were then adjusted and the error limits obtained using the automated FITSIM routine that calculates the best values by minimization of the difference between the experimental and simulated data using an iterative nonlinear least-squares procedure. The standard error for each individual rate constant has been estimated to be less than 15% using the FITSIM program.

Determination of Aldehyde Hydration Constant. The equilibrium constant and rate of dehydration of *n*-octanal were determined enzymatically using horse liver alcohol dehydrogenase as described by Deetz et al. (*24*). The equilibrium constant for the hydration reaction and the rate constants for the hydration and dehydration reactions were determined for 1-[^{1}H]octanal and 1-[^{2}H]octanal in 50 mM TES buffer solutions made with either H_2O or D_2O at 25 °C, pH 7.0. The *n*-octanal stock solutions were prepared in acetonitrile and the hydrated solutions were obtained by equilibration following a 5-fold dilution of the aldehyde-acetonitrile solution with TES buffer.

pH Rate Profiles. The pH dependence of enzymatic activity and the rate of decay of light emission were studied using 1-[^{1}H]decanal and 1-[^{2}H]decanal as substrates. The activity was measured using the standard assay (*25*) in 25 mM Tris-maleate buffer solutions at 25 °C as a function of pH as described by Nicoli et al. (*26*). The pH range was from 6.0 to 9.0. The reaction was initiated by vigorous injection of 1.0 mL of a catalytically reduced 50 μM solution of $FMNH_2$ into a vial containing 1.0 mL of 25 mM Tris-maleate buffer at the desired pH containing luciferase (0.1 μM) and either 1-[^{1}H]decanal or 1-[^{2}H]decanal (50 μM). This concentration of aldehyde was found to be optimal and no aldehyde substrate inhibition was observed. The pK_a values were determined by fitting the data to one of the following equations:

$$\log k = \log[C/(1 + H/K_a)] \quad (6)$$

$$\log k = \log[C/(1 + H/K_a + K_b/H)] \quad (7)$$

where k is either the initial maximum light intensity (I_{max}) or the rate constant for the decay of light emission (k_d), C is the pH-independent value of I_{max} or k_d, H is the hydrogen ion concentration, and K_a and K_b are the dissociation constants of the ionizable groups.

Theoretical Calculations. The fully optimized structures reported here were obtained with Gaussian 94 (*27*). (U)-MP2 geometry optimizations and (U)MP4(STDQ) single-point energies were performed as implemented in Gaussian 94, with core orbitals frozen. A 6-31+G** basis set was used for all calculations. Vibrational frequency analyses were carried out on all stationary points. Reduced isotopic

Table 1: Deuterium Kinetic Isotope Effects for the Luciferase Catalyzed Reaction[a]

enzyme	experiment	$^{D}I_{max}$	$^{D}k_{d}$	^{D}Q
wild-type	E·$FMNH_2$ vs O_2·decanal	1.51 ± 0.09	1.50 ± 0.06	1.01 ± 0.07
wild-type	E·O_2·decanal vs $FMNH_2$	1.53 ± 0.10	1.45 ± 0.04	1.04 ± 0.07
wild-type	E·$FMNH_2$ vs O_2·octanal	1.46 ± 0.05	1.47 ± 0.11	0.98 ± 0.09
wild-type	E·$FMNH_2$ vs O_2·dodecanal	1.36 ± 0.09	1.39 ± 0.03	0.98 ± 0.07
C106A	E·$FMNH_2$ vs O_2·decanal	1.74 ± 0.05	1.46 ± 0.08	1.19 ± 0.07
C106S	E·$FMNH_2$ vs. O_2·decanal	1.78 ± 0.09	1.39 ± 0.08	1.28 ± 0.10
C106V	E·$FMNH_2$ vs O_2·decanal	1.55 ± 0.08	0.87 ± 0.11	1.78 ± 0.24
wild-type	E·8-Cl-$FMNH_2$ vs O_2·decanal	1.84 ± 0.11	1.46 ± 0.09	1.26 ± 0.11
wild-type	E·8-CH_3O-$FMNH_2$ vs O_2·decanal	1.50 ± 0.25	0.95 ± 0.06	1.58 ± 0.28

[a] Reaction conditions: pH 7.0, 25 °C. $^{D}I_{max}$ is the deuterium isotope effect on the maximum light intensity, $^{D}k_{d}$ is the deuterium isotope effect on the decay rate of the emitted light, and ^{D}Q is the deuterium isotope effect on the quantum yield.

partition functions and isotope effects were calculated by the method of Bigeleisen and Mayer (*28*−*30*) using the program QUIVER (*31*), with frequencies unscaled.

RESULTS

Isotope Effects on Light Production. Plots of the relative maximum light intensity (I_{max}) and the decay rate for light emission (k_d) versus the initial aldehyde concentration when a solution of enzyme and $FMNH_2$ was mixed with air-equilibrated solutions of either 1-[^{1}H]decanal or 1-[^{2}H]-decanal are shown in Figure 3, panels A and B. The maximum light intensity increased as the aldehyde concentration was elevated until it reached a maximum value at around 200 μM and then remained constant at higher concentrations of aldehyde. The first-order rate constant for the decay of light emission also exhibited a similar behavior, reaching a constant value of 0.50 s^{-1} for 1-[^{1}H]decanal and 0.33 s^{-1} for 1-[^{2}H]decanal at high concentrations of aldehyde. The maximum light intensity was diminished and the decay of the light emission was slower when 1-[^{2}H]decanal was used as the substrate. An isotope effect of 1.5 was observed for both parameters throughout the entire aldehyde concentration range. No isotope effect was observed on the quantum yield (Q), defined as the total quanta produced under nonturnover conditions, or simply estimated as the ratio of the maximum light intensity and the rate of light decay (I_{max}/k_d).

The maximum light intensity and associated decay rate were also measured after aerobic solutions of enzyme and varying concentrations of either 1-[^{1}H]decanal or 1-[^{2}H]-decanal were mixed with $FMNH_2$ (Figure 3, panels C and D). In this type of assay, a reduced enzyme activity was observed at high concentrations of aldehyde. The decay rate of the emitted light exhibited the same type of behavior as in the experiment described above; the rate of light decay increased slightly as the concentration of aldehyde was raised until it obtained a constant value of 0.48 s^{-1} for 1-[^{1}H]decanal and 0.33 s^{-1} for 1-[^{2}H]decanal at high concentrations of aldehyde. An isotope effect of 1.5 was observed on the maximum light intensity and the decay rate of the emitted light throughout the entire aldehyde concentration range. These results are summarized in Table 1.

Deuterium Isotope Effects as a Function of Aldehyde Chain Length. The deuterium isotope effects on the maximum light intensity and the decay rate for light emission were also determined for *n*-octanal and *n*-dodecanal. The maximum light intensity observed with these two aldehydes was approximately 10% of that observed with *n*-decanal, and the rate of decay of the emitted light was approximately 10-fold slower. When solutions of enzyme and $FMNH_2$ were mixed with air-equilibrated solutions of either 1-[^{1}H]octanal or 1-[^{2}H]octanal, the maximum light intensity increased as the aldehyde concentration was elevated up to 200 μM and remained constant at higher concentrations of aldehyde (data not shown). The decay rate for light emission decreased slightly as the aldehyde concentration was increased and reached a limiting value of 0.050 s^{-1} for 1-[^{1}H]octanal and 0.034 s^{-1} for 1-[^{2}H]octanal at an aldehyde concentration of approximately 200 μM. An isotope effect of 1.5 was observed for both the maximum initial light intensity and the decay rate of light emission. No isotope effect was observed for the quantum yield. The activity profiles for the assays where *n*-dodecanal was used as a substrate were very similar to those observed with *n*-octanal, with the only difference being that lower concentrations of *n*-dodecanal were needed to reach a saturation point ($\leq$50 μM). An isotope effect of 1.4 was observed for both the maximum light intensity and the decay rate of light emission when solutions of enzyme and $FMNH_2$ were mixed with aerobic solutions of *n*-dodecanal (data not shown). These results are also summarized in Table 1.

Deuterium Isotope Effects for α*C106 Mutants.* The chemically reactive cysteine residue at position 106 of the α subunit of luciferase has been replaced with serine, alanine, and valine (*11*). All three mutants catalyze the emission of visible light, but the maximum light intensities and light decay rates are different from those of the wild-type enzyme. The isotope effects on the maximum light intensity and on the decay rate of the emitted light were measured for these three mutants in both assay formats using *n*-decanal as the substrate.

The relative maximum light intensity of the αC106A mutant was approximately 60% of that of the wild-type enzyme and the decay rate was approximately 1.7-fold slower. The activity profiles for this enzyme were very similar to those of the wild-type enzyme. When a solution of enzyme and $FMNH_2$ was mixed with air-equilibrated solutions of *n*-decanal, the maximum light intensity increased as the concentration of aldehyde was increased, reaching a maximum at about 100 μM decanal (data not shown). The light decay rate decreased slightly as the aldehyde concentration was raised, reaching a limiting value of 0.30 s^{-1} for 1-[^{1}H]decanal and 0.20 s^{-1} for 1-[^{2}H]decanal at approximately 100 μM decanal (data not shown). The observed isotope effects for the maximum light intensity and the light decay rate were 1.7 and 1.5, respectively. The maximum

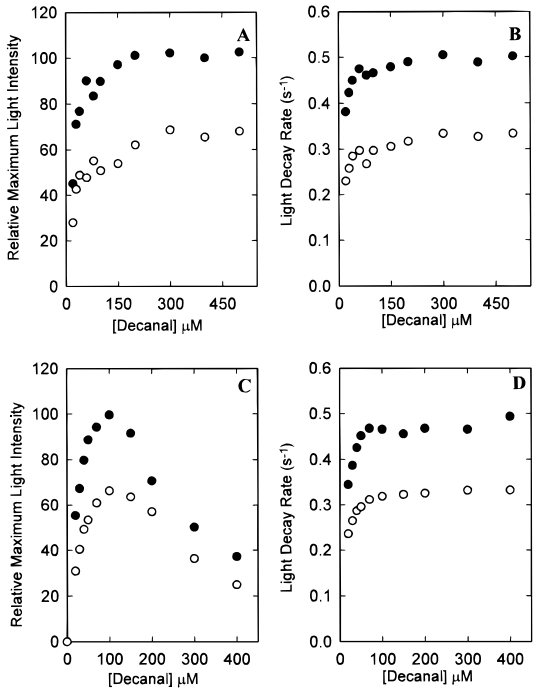

FIGURE 3: Isotope effect on the maximum light intensity and decay rate for light emission for wild-type luciferase with *n*-decanal. Maximum light intensities (A) and light emission decay rates (B) for the reaction of enzyme (75 μM) and $FMNH_2$ (15 μM) with various amounts of 1-[^{1}H]decanal (●) and 1-[^{2}H]decanal (○). Maximum light intensities (C) and decay rates (D) for the reaction of enzyme and various amounts of 1-[^{1}H]decanal (●) and 1-[^{2}H]-decanal (○) in air-equilibrated buffer with $FMNH_2$. The final concentrations of enzyme and $FMNH_2$ were 75 and 15 μM, respectively.

light intensity observed with the αC106S mutant was approximately 30% of that for the wild-type enzyme, and the decay rate of the emitted light was approximately 1.3-fold faster. The activity profiles for this mutant when solutions of enzyme and $FMNH_2$ were mixed with aerobic solutions of *n*-decanal exhibited an isotope effect of 1.8 for the maximum light intensity and 1.4 for the light decay rate.

The αC106V protein was the dimmest of the mutants used. The maximum light intensity was only 2% of the wild-type enzyme. The activity profiles for this mutant when solutions of enzyme and $FMNH_2$ were mixed with aerobic solutions of *n*-decanal are shown in Figure 4. The light decay rate for this enzyme was quite dependent on the aldehyde concentration. The rate constant for the decay of the emitted light decreased from around 2.4 s^{-1} at low levels of *n*-decanal (30 μM) to around 0.6 s^{-1} at high levels of *n*-decanal (500 μM) (Figure 4B). An isotope effect of 1.6 was observed for the maximum light intensity when solutions of enzyme and $FMNH_2$ were mixed with aerobic solutions of decanal (Figure 4A). Very interestingly, the observed isotope effect for the decay of the emitted light was very near unity or slightly inverse. A summary of the results obtained with the αC106 mutants is presented in Table 1.

Isotope Effect for 8-X-FMNH$_2$ Derivatives. Several 8-substituted $FMNH_2$ derivatives have been shown to be substrates for the luciferase-catalyzed reaction (*32*). The maximum light intensity and the decay rate of light emission for these derivatives are very different relative to those observed with $FMNH_2$ (*32*). The isotope effects on the maximum light intensity and on the light emission decay

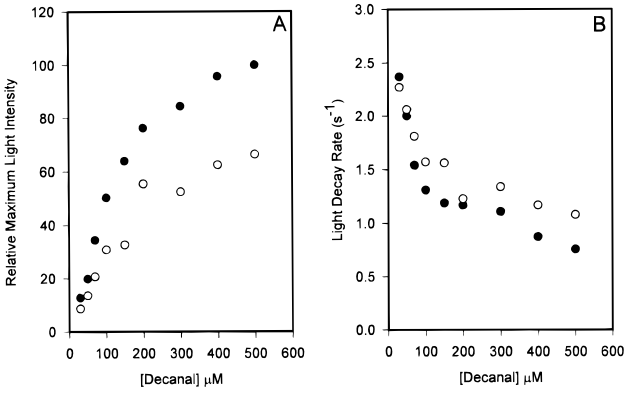

FIGURE 4: Deuterium isotope effect on the maximum light intensity and decay rate of light emission for the αC106V mutant of luciferase with *n*-decanal. Maximum light intensities (A) and light emission decay rates (B) for the reaction of enzyme (75 μM) and $FMNH_2$ (15 μM) with various amounts of 1-[^{1}H]decanal (●) and 1-[^{2}H]decanal (○).

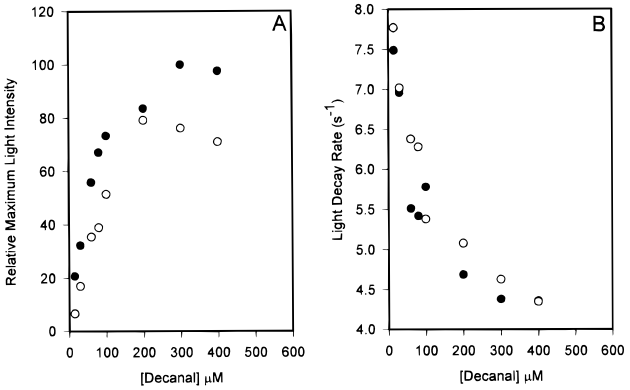

FIGURE 5: Deuterium isotope effect on the maximum light intensity and decay rate of light emission for wild-type luciferase with 8-CH_3O-$FMNH_2$. Maximum light intensities (A) and light emission decay rates (B) for the reaction of enzyme (75 μM) and 8-CH_3O-$FMNH_2$ (15 μM) with various amounts of 1-[^{1}H]decanal (●) and 1-[^{2}H]decanal (○).

Table 2: Hydration Constants for *n*-Octanal in Aqueous Solutions[a]

solvent	aldehyde	k_f (min^{-1})	k_r (min^{-1})	K_{eq}
H_2O	1-[^{1}H]octanal	0.17 ± 0.02	0.34 ± 0.02	0.49 ± 0.03
H_2O	1-[^{2}H]octanal	0.20 ± 0.02	0.33 ± 0.02	0.62 ± 0.03
D_2O	1-[^{1}H]octanal	0.056 ± 0.01	0.11 ± 0.01	0.52 ± 0.05

[a] TES (50 mM).

rates were determined for 8-Cl-$FMNH_2$ and 8-CH_3O-$FMNH_2$ when the enzyme was assayed by mixing solutions of enzyme and reduced flavin analogues with *n*-decanal.

The decay rate of light emission for the 8-Cl-$FMNH_2$ derivative was 20-fold slower than with $FMNH_2$. The activity profiles for the 8-Cl-$FMNH_2$ derivative exhibited a deuterium isotope effect of 1.8 for the maximum light intensity and 1.5 for the decay rate (data not shown). The activity profiles for the 8-CH_3O-$FMNH_2$ derivative are shown in Figure 5. The rate of decay of light emission for the 8-CH_3O-$FMNH_2$ derivative was approximately 9 times faster than for $FMNH_2$. The rate of decay for light emission with this derivative was very dependent on the total aldehyde concentration. The rate constant for the decay of light emission at low *n*-decanal concentrations was approximately 7.5 s^{-1} (15 μM) and 4.3 s^{-1} at high *n*-decanal concentrations (500 μM) (Figure 5B). No significant isotope effect was

observed for the light emission decay rate. A summary of the results obtained for the 8-substituted flavin derivatives is presented in Table 1.

Hydration-Dehydration of Aldehydes. It is known that in aqueous solutions, aldehydes exist as a mixture of the hydrated and unhydrated species, as shown below:

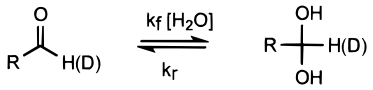

The extent of aldehyde hydration and the rates of the hydration and dehydration reactions for *n*-octanal were determined using horse liver alcohol dehydrogenase for the direct measurement of the unhydrated species (*24*). The enzymatic assays were done with 1-[^{1}H]octanal and 1-[^{2}H]-octanal in H_2O and D_2O solutions. An equilibrium constant for the hydration reaction (K_{eq} = [*gem*-diol]/[aldehyde]) of 0.49 ± 0.03 was measured for 1-[^{1}H]octanal and 0.62 ± 0.03 for 1-[^{2}H]octanal in H_2O solutions. This represents an inverse equilibrium isotope effect ($^DK_{eq} = K_H/K_D$) of 0.79. The rate constants for hydration (k_f) and dehydration (k_r) of 1-[^{1}H]octanal were 0.17 ± 0.02 min^{-1} and 0.34 ± 0.02 min^{-1}, respectively. For 1-[^{2}H]octanal, the rates of hydration and dehydration were 0.20 ± 0.02 min^{-1} and 0.33 ± 0.02 min^{-1}, respectively. The deuterium kinetic isotope effects (^Dk_f and ^Dk_r) for the hydration and dehydration rate constants were 0.85 ± 0.10 and 1.06 ± 0.09, respectively. When D_2O was used as the solvent, the equilibrium constant for the hydration reaction was found to be 0.52 ± 0.05 for 1-[^{1}H]-octanal. The rates of hydration and dehydration in D_2O for 1-[^{1}H]octanal are 0.056 ± 0.008 min^{-1} and 0.11 ± 0.01 min^{-1}, respectively. These results are summarized in Table 2.

*pH Profiles.*The luciferase-catalyzed enzymatic activity was measured as a function of pH using the standard assay format in Tris-maleate buffer solutions over the pH range of 6.0−9.0. The maximum light intensity and the decay rate of the emitted light were measured at a constant aldehyde concentration at 0.25 pH-unit intervals using either 1-[^{1}H]-decanal or 1-[^{2}H]decanal as substrates. The pH profiles for the emission of visible light for both 1-[^{1}H]decanal and 1-[^{2}H]decanal are shown in Figure 6A. The pK_a values of the ionizable groups were determined from the pH dependence of I_{max} by fitting the data to eq 7. The pK_a values determined when 1-[^{1}H]decanal was used as a substrate were 6.9 ± 0.1 and 8.2 ± 0.1. The pK_a values determined when 1-[^{2}H]decanal was used as a substrate were 6.7 ± 0.1 and 8.4 ± 0.1. The pH profiles for the decay rate of light emission for both 1-[^{1}H]decanal and 1-[^{2}H]decanal are shown in Figure 6B. The rate of light emission remained almost constant in the pH range 6−7.5 and then decreased as the pH increased. The pH dependencies of the decay rate for both 1-[^{1}H]decanal and 1-[^{2}H]decanal were fit to eq 6. A pK_a of 8.1 ± 0.1 was determined when 1-[^{1}H]decanal was used as a substrate and 8.2 ± 0.1 when 1-[^{2}H]decanal was used.

Solvent Isotope Effects. The effect of deuteration of the solvent was studied for various reactions. No measurable effect was observed on either the rate of autoxidation of $FMNH_2$ or the formation and decay of the C4a-hydroperoxyflavin intermediate. The effect of deuteration was also

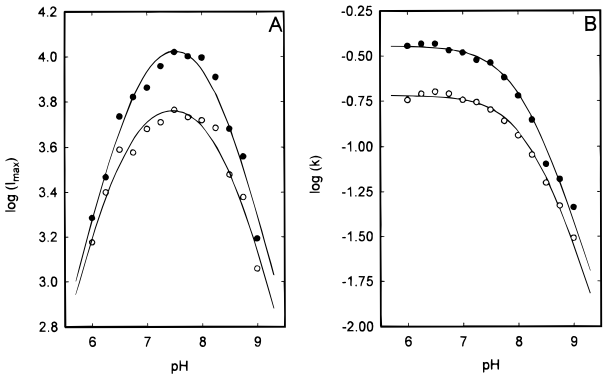

FIGURE 6: The pH profile for the maximum light intensity and decay rate of light emission of bacterial luciferase. pH profiles of the maximum light intensity (A) and decay of light emission (B) determined using the standard assay with 1-[^{1}H]decanal (●) and 1-[^{2}H]decanal (○) as substrates. The solid lines in panel A were drawn from a fit of the data to eq 7 and the solid lines in panel B were drawn from a fit of the data to eq 6. Additional details are given in the text.

Table 3: Rate Constants for the Kinetic Model in Figure 2 for the Substrate *n*-Decanal[a]

rate constant	1-[^{1}H]decanal	1-[^{2}H]decanal
k_7	3.0 × 10^7 M^{-1} s^{-1}	3.0 × 10^7 M^{-1} s^{-1}
k_8	110 s^{-1}	110 s^{-1}
k_9	3.3 s^{-1}	4.1 s^{-1}
k_{10}	0.80 s^{-1}	0.76 s^{-1}
k_{11}	0.65 s^{-1}	0.35 s^{-1}
k_{25}	0.0028 s^{-1}	0.0033 s^{-1}
k_{26}	0.0057 s^{-1}	0.0055 s^{-1}

[a] pH 7.0, 25 °C. The rate constants k_1 (1.0 × 10^7 M^{-1} s^{-1}), k_2 (75 s^{-1}), k_3 (200 s^{-1}), k_4 (14 s^{-1}), k_5 (2.4 × 10^6 M^{-1} s^{-1}), k_{13} (0.6 s^{-1}), k_{17} (0.1 s^{-1}), k_{21} (4.47 s^{-1}), and k_{23} (11.2 s^{-1}) have been reported elsewhere (*11*).

measured for the decay rate of light emission for 1-[^{1}H]-decanal and 1-[^{2}H]decanal. When an H_2O solution of enzyme (75 μM) and $FMNH_2$ (15 μM) was mixed with an aerobic solution of *n*-decanal (200 μM), a rate constant for the decay of the emitted light of 0.50 s^{-1} was observed with 1-[^{1}H]decanal and 0.30 s^{-1} for 1-[^{2}H]decanal. When the same experiment was performed in 95% D_2O, a rate constant of 0.36 s^{-1} was measured for 1-[^{1}H]decanal and 0.20 s^{-1} for 1-[^{2}H]decanal.

Calculation of Microscopic Rate Constants. The microscopic rate constants for the kinetic model that appears in Figure 2 for 1-[^{1}H]decanal and 1-[^{2}H]decanal with wild-type luciferase and $FMNH_2$ are presented in Table 3. These rate constants were obtained by direct comparison of the experimental time courses for light production with the calculated time courses using the KINSIM program. The rate constants for the hydration of the aldehyde (k_{25} and k_{26}) were those obtained for the case of *n*-octanal. The rate constants for the formation (k_1 to k_5) and decay (k_{17}) of E′•FMNOOH, the rate of decomposition of E′•FMNOH (k_{13}, k_{15} and k_{16}), and the rate of autoxidation of $FMNH_2$ have been reported previously (*10, 11*) and were held constant during the simulation.

The rate constants associated with the binding of aldehyde to free enzyme (k_{19} and k_{20}) and the rate constants for the processes associated with the binding of aldehyde to the E′•FMNOOH complex through the formation of E′•FMNOH (k_7 to k_{11}) were established by the simultaneous fit of the

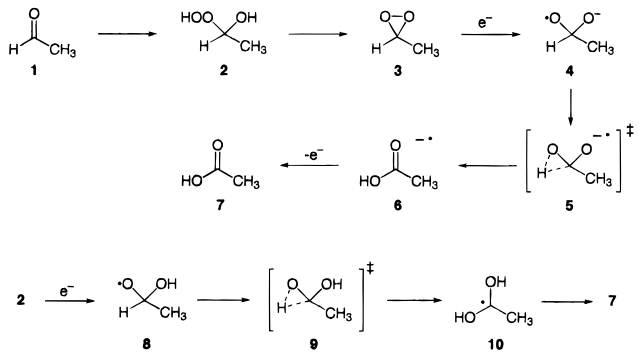

FIGURE 7: Calculational model mechanism for the bacterial luciferase reaction.

Table 4: Energies, Isotopic Fractionation Factors, and Isotope Effects for Calculated Structures

structure	(U)MP2	(U)MP4 (SDTQ)	reduced isotopic partition function[a]	calculated isotope effect[b]
1	−153.38908		12.000	
2	−304.58454		17.390	0.69[c]
3	−228.32326	−228.37395	16.214	1.07[d]
4	−228.36467	−228.42134	9.268	1.88[d]
5	−228.36258	−228.41855	3.662	4.8[e]
6	−228.41115	−228.46052		
7	−228.46999	−228.51732		
8	−228.95943	−229.01718	14.063	1.24[d]
9	−228.91988	−228.97332	4.784	4.9[e]
10	−228.98111	−229.03208		

[a] Temperature 25 °C. [b] Equilibrium isotope effects were calculated from the ratio of reduced isotopic partition functions. Kinetic isotope effects also include a factor for the ratio of calculated imaginary frequencies for isotopomers at the transition state (*28*). [c] Equilibrium isotope effect (k_H/k_D) predicted for formation from acetaldehyde (**1**). [d] Equilibrium isotope effect for formation from **2**. [e] Kinetic isotope effect based on **2** as the starting material.

time courses for the emission of visible light that followed the mixing of air-equilibrated aldehyde with a mixture of enzyme and $FMNH_2$ and those obtained when $FMNH_2$ was mixed with a solution of enzyme and aldehyde to the kinetic model that appears in Figure 2.

The time courses for the reactions with 1-[^{1}H]decanal were simulated first. The rate constants obtained for 1-[^{1}H]decanal were used, after some modifications, as initial estimates for the simulation of the light emission profiles obtained with 1-[^{2}H]decanal. The modifications were based on the known deuterium isotope effects on the individual rate constants. The values utilized for the rates of aldehyde hydration and dehydration were those obtained for 1-[^{2}H]octanal (see Table 2). An equilibrium isotope effect for the formation of E′·FMNOOR from the E′·FMNOOH·RCHO is expected, and the respective rate constants (k_9 and k_{10}) were multiplied by the factor obtained from the rate constants for aldehyde hydration and dehydration for 1-[^{1}H]octanal and 1-[^{2}H]-octanal. No deuterium isotope effect was anticipated for the binding of the aldehyde to the E′·FMNOOH complex, and these rate constants were held constant during the simulation of the 1-[^{2}H]decanal data.

Theoretical Results. Figure 7 shows two model mechanisms examined in ab initio calculations. The first is based on the proposed intermediacy of a dioxirane (*33*, *34*) while the second is based on the direct cleavage of FMNOOR on electron transfer as proposed by Eckstein et al. (*32*). In these calculational models, the long alkyl chain of the starting aldehyde, final acid, and all intermediates was replaced by a methyl group, and 1-hydroxyethyl hydroperoxide (**2**) was used to model FMNOOR. Stationary points corresponding to the radical anion of methyldioxirane (**3**) and the transition state for its ring opening could not be located, apparently the O−O bond of methyldioxirane is broken without barrier on reduction to afford the dioxyethane radical anion **4**. A transition structure (**5**) was located for the rearrangement of **4** to acetic acid radical anion. This rearrangement is predicted to be exothermic by 24.6 kcal/mol at the UMP4/6-31+G**//UMP2/6-31+G** level with a barrier of only 1.7 kcal/mol, while the barrier to rearrangement of **8** to **10** via transition structure **9** predicted at the same level is 27.5 kcal/mol. The overall rearrangement of methyldioxirane to acetic acid is predicted to be exothermic by 90.0 kcal/mol. The energies of the series of intermediates and transition states in the model mechanisms are summarized in Table 4, along with the calculated reduced isotopic partition functions for substitution of deuterium for hydrogen in each structure at the position corresponding to the aldehydic C−H, and appropriate calculated isotope effects.

DISCUSSION

The discussion here will first try to pin down the nature of the isotope effects observed in the bacterial luciferase reaction, then use the isotope effects in concert with theoretical calculations and other observations to formulate a consistent detailed molecular mechanism.

Isotope Effects. In the critical mechanistic steps between the time of formation of the hydroperoxy hemiacetal and the formation of the excited state of the flavin pseudo-base (Figure 1), the fate of the aldehydic hydrogen has not been defined. Since this atom is ultimately found in the solvent, the C−H bond of the aldehyde must be broken sometime during the course of the overall reaction. However, it has not yet been ascertained whether the C−H bond cleavage is heterolytic or homolytic, or if the bond breakage is part of the rate-limiting step(s). One approach to this problem is to measure kinetic isotope effects upon substitution of a deuterium for protium at this site within the aldehyde substrate. However, all previous investigations of the deuterium isotope effects on the decay of luminescence have obtained a value of approximately 1.5 when *n*-decanal and $FMNH_2$ were used as substrates. This modest value is larger than normal α-secondary effects and is significantly smaller than expected for a primary deuterium kinetic isotope effect.

The series of chemical steps that must occur prior to the emission of visible light from the active site of luciferase is reasonably complex. The actual size of any apparent kinetic isotope effect may, in fact, be modulated by the nature of the chemical events and the sequence of transformations leading up to the moment for actual light emission. For example, an inverse secondary equilibrium isotope effect of about 0.80 is expected on the formation of the hydroperoxy hemiacetal (*35*). This α-secondary isotope effect is due to the change in bond stiffness that accompanies the change in hybridization of the carbonyl carbon from sp^2 to sp^3. An estimate for the magnitude of this effect in the luciferase catalyzed reaction was made by determining the deuterium isotope effect on the equilibrium constant for the hydration

of *n*-octanal to the corresponding *gem*-diol. The experimental α-secondary deuterium effect on the equilibrium constant for this reaction with *n*-octanal is 0.79. An isotope effect of similar size would also be anticipated for the analogous addition of the hydroperoxide intermediate to the carbonyl group of the aldehyde substrate. This inverse effect (whether kinetic or equilibrium) would then tend to diminish the observed effect of isotopic substitution on the decay of light emission. The small spectral changes in the flavin nucleus observed by Macheroux et al. (*4*) during substrate binding and turnover have provided direct spectral support for the formation of an intermediate prior to the excited state. These absorbance changes are formed with an apparent inverse isotope effect of 0.90 and 0.75 when *n*-octanal and *n*-dodecanal, respectively, are used as substrates.[2] However, these inverse α-secondary isotope effects were not recognized at the time (*4*) but, in fact, supply the best direct evidence for the formation of the hydroperoxy hemiacetal intermediate during the luciferase catalyzed reaction. Our simulations of the time courses for light emission are fully consistent with an inverse isotope effect during the formation of this intermediate.

Our calculations indicate that the deuterium kinetic isotope effect on the decay of light emission (k_{11}) is 1.9 for *n*-decanal with $FMNH_2$. In the mechanism presented in Figure 2, the step depicted by the rate constant k_{11} is a composite for a number of steps that occur after the formation of the hydroperoxy hemiacetal. It is not clear whether this rate constant represents a single rate-limiting mechanistic step or multiple rate-limiting steps. Therefore, the calculated kinetic isotope effect of 1.9 might represent an intrinsic isotope effect or, alternatively, might be the result of a larger primary isotope effect diminished due to the mechanistic and kinetic complexities of the luciferase catalyzed reaction. One approach to simplify these apparent complexities has been articulated by Cleland (*6*) and involves the measurement of isotope effects with modified substrates, extremes of pH and the utilization of sluggish mutants of the native enzyme. These changes in reaction conditions can be utilized for the purpose of altering the rate-limiting step(s) and/or modulating the structure of the transition state. Therefore, we have utilized this approach to exploit the information that can be extracted from the use of heavy atom isotopes to elucidate the mechanism for light emission in the bacterial luciferase catalyzed reaction.

Variation of the Aldehyde Chain Length. The apparent deuterium kinetic isotope effects were first measured using deuterated aldehydes of different carbon chain lengths. Quite curiously, changing the carbon length from C-10 to C-8 and C-12 alters the rate constants for light emission from 0.50 to 0.05 s^{-1} and 0.034 s^{-1}, respectively. The changes in rate constant may originate from the nonproductive binding of aldehydes of different chain length. These are substantial effects considering that the additional methylene groups are being added to the substrate at a position rather remote from the carbonyl group of the *n*-decanal parent. This reduction in the decay rate for light emission is not, however, accompanied by any significant change in the observed deuterium isotope effect. This observation must mean that either the change in aldehyde chain length has diminished equally all of the rate-limiting steps after the formation of the hydroperoxy hemiacetal or, alternatively, that there is a single rate-limiting step.

Variation of the Flavin Structure. The change in the redox potential and electron-withdrawing properties of the reduced flavin substrate was also used in an attempt to modulate the magnitude of the observed deuterium kinetic isotope effect. With an electron-withdrawing chloride substituent at the 8-position of the flavin, the rate of decay for light emission is 20-fold slower than with a methyl substituent at this same position. However, the observed deuterium isotope effect on the decay of light emission is essentially unchanged relative to $FMNH_2$ itself. Since the substantial reduction in the rate of decay of light emission observed with the electron-withdrawing substituent has been proposed to be due to a requirement for an electron transfer from the flavin to the aldehyde/acid (*32*), then the constancy of the deuterium isotope effect with the flavin substrate would argue that the isotope effect is associated with the electron-transfer process as a single rate-limiting step. Otherwise, the observed isotope effect would be anticipated to diminish in magnitude with the slower substrate, but this is not observed. In support of this conclusion are the results obtained with the methoxy substituent at this same site in the flavin nucleus. The rate constant for the decay of light emission with the 8-MeO-$FMNH_2$ is an order of magnitude faster than with $FMNH_2$. The observed deuterium isotope effect is 0.95 (slightly inverse). With this faster substrate, the apparent electron-transfer step is no longer as rate limiting as with the native $FMNH_2$. If the electron-transfer step and a step having a large primary isotope effect (i.e., C−H bond cleavage) occurred sequentially in partially rate-limiting steps, then the observed isotope effect would have been predicted to increase. The reduction in the observed isotope effect is therefore consistent with a single rate-limiting step after the formation of the hydroperoxy hemiacetal. With the 8-MeO-$FMNH_2$ analogue, it is tempting to speculate that the formation of the hydroperoxy hemiacetal has now become partially rate limiting since a slightly inverse effect is observed.

Variation of the Active-Site Residues. Site-directed mutants of active-site residues of bacterial luciferase were utilized to probe the origin of the deuterium isotope effects. The best characterized of these mutants are those constructed for the chemically reactive residue at αC106 (*11*). The mutants, αC106A and αC106S, have rate constants for the decay of light emission that are 1.7-fold slower and 1.3-fold faster, respectively, than the wild-type enzyme. Although these changes in rate are rather modest, there is no observable effect on the measured deuterium kinetic isotope effects (1.5 and 1.4, respectively). However, a significantly different picture emerges with the αC106V mutant. The observed deuterium isotope effect on the decay of light emission is slightly inverse, but the observed quantum yield is only 2% that of the wild-type enzyme under identical reaction conditions. The decay rate is slightly faster (0.6 versus 0.5 s^{-1}). Why is the deuterium isotope effect so low when the apparent decay rate for light emission is identical

[2] The apparent isotope effects for the first phase of the absorbance changes in the visible region of the spectrum during the luciferase-catalyzed reaction were calculated from the half-times reported in Table 1 of Macheroux et al. (*4*). For *n*-octanal the deuterium isotope effect is 0.90 (210 s/235 s) and for *n*-dodecanal the deuterium isotope effect is 0.75 (150 s/ 200 s).

with the wild-type enzyme? Previous characterization of the kinetic behavior of the αC106V mutant has clearly demonstrated that the decay of light intensity is *not* limited by k_{11} (*11*). The observed value is an artifact that is the direct result of an extremely unstable hydroperoxide intermediate and a rather unfavorable equilibrium constant for the formation of the hydroperoxy hemiacetal (*11*). Thus, the low quantum yield is due to a dominant off-pathway dark reaction that masks any intrinsic isotope effect on the actual step for light formation.

Alteration in pH. The deuterium isotope effects on the maximum light intensity and on the decay rate for light emission were measured as a function of pH. At a fixed aldehyde concentration, there is observed a bell-shaped pH profile for the maximum emitted light intensity. The maximum light intensity drops off at both high and low pH, but the observed deuterium isotope effect does not vary significantly over the pH range 6−9. The drop in the quantum yield at low pH (with a pK_a of 6.9) is proposed to be due to the protonation of the reduced flavin. The pK_a value for the hydrogen at N1 of $FMNH_2$ is 6.2. Either the protonated $FMNH_2$ species does not bind to the enzyme or the protonated species does not react with molecular oxygen on the enzyme to form the hydroperoxide intermediate at a significant rate. In these single turnover experiments, either of these effects would result in the reduction in the observed light intensity and apparent quantum yield. At higher pH values, the I_{max} values and the decay rates for light emission decrease together, and thus, the apparent quantum yield is relatively constant. The drop in the light decay rate at high pH may be the result of ionization of a residue that protonates or hydrogen bonds to the light-emitting complex prior to the rate-limiting step.

If a proton transfer is involved in the rate-limiting step prior to the emission of visible light, then one might expect to observe a significant solvent isotope effect on the decay rate of light emission. When the luciferase catalyzed reaction is conducted in 95% D_2O, an isotope effect of 1.4 is observed on the decay rate of light emission using 1-[^{1}H]decanal as a substrate and 1.5 using 1-[^{2}H]decanal as a substrate. These modest isotope effects are consistent with proton-transfer equilibria before the rate-limiting step.

The Molecular Mechanism of Luciferase Luminescence. In sum, the observations above strongly support the contention that the isotope effect on k_{11} of 1.9 is the result of a change in rate of a single kinetic step. Any mechanism proposed for the central steps in luciferase luminescence should account for this isotope effect as well as the observed correlation of the decay rate for light emission with the redox potential of the dihydroflavin. It was noted by Eckstein et al. (*32*) that a Baeyer−Villiger type mechanism (*36*, *37*) would predict a wrong trend for rate versus redox potential. We note here that a Baeyer−Villiger type mechanism (Figure 8) also does not account for the observed isotope effects since a large primary effect would be expected.

Two other mechanisms based on previous proposals are shown in Figures 9 and 10. The first involves the proposed dioxirane intermediate (*33*, *34*). Rate-limiting electron transfer to the dioxirane in **12** to form **13** would be consistent with the observed correlation of rate with dihydroflavin redox potential. This is also true of the mechanism of Figure 10 involving a direct electron transfer within FMNOOR to

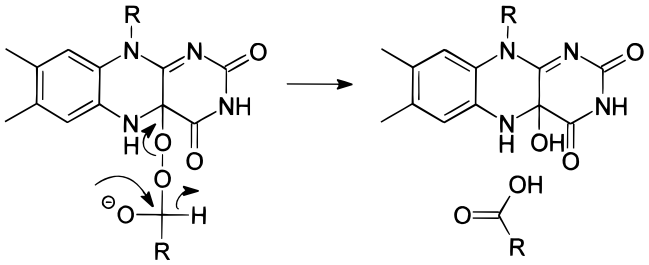

FIGURE 8: A Baeyer−Villiger mechanism for the luciferase catalyzed reaction.

cleave the O−O bond and form **16**, as proposed by Eckstein et al. (*32*). However, a critical problem was that it was unclear how these mechanisms or any other mechanism could account for the aldehyde isotope effect.

A key insight in this regard came with the observation that the reduced isotopic partition function calculated for the radical anion **4** is anomalously low for H/D on an sp^3 carbon. This low fractionation factor is related to the very low barrier predicted for 1,2-hydrogen migration in **4**, in that the C−H stretching frequency in **4** is quite low [2556 cm^{-1} compared to 3120 cm^{-1} in **2** (the calculated frequencies are unscaled)]. The result is that the calculated *equilibrium* isotope effect for formation of **4** from **2** is 1.88. This is extraordinarily high for a secondary isotope effect but is understandable if one views **4** as having, in effect, a partially broken C−H bond.

The predicted *kinetic* isotope effect if electron transfer to **3** to form **4** is rate limiting depends on the energetics of the electron transfer. Since there is no barrier predicted for ring opening of the radical anion of the dioxirane **3** to form **4**, this conversion may be considered a single kinetic step. In the actual system (electron transfer in **12** to form **13**), it is reasonable to assume that this step is moderately endothermic, if it were thermoneutral or exothermic, a different trend in rate versus redox potential of the dihydroflavin would be expected, and the electron transfer would likely be too fast to be rate limiting. The equilibrium isotope effect for a reaction is equal to the ratio of kinetic isotope effects for the forward and reverse reactions, i.e., $K_H/K_D = k_H/k_D$(forward)/ k_H/k_D(reverse). For highly exothermic electron transfers, k_H/k_D increases as ΔG_{et} increases in the Marcus "inverted region", but this quantum effect falls off to unity for moderately exothermic electron transfers (*38*). Thus, for a moderately endothermic electron transfer, k_H/k_D(reverse) ∼1. The expected kinetic isotope effect for electron transfer to **3** to form **4** would then be equal to the equilibrium isotope effect of 1.88. This is in excellent agreement with the observed isotope effect on k_{11} of 1.9, indicating that the unusual experimental isotope effect is consistent with rate-limiting electron transfer in **12** to form **13**.

The direct electron-transfer-mediated cleavage of FMNOOR in Figure 10 might be expected to exhibit a similar isotope effect since **16** differs from **13** only by the position of a proton. However, the presence of an extra proton in the theoretical model **8**, compared to **4**, raises the predicted barrier to 1,2-rearrangement in **8** to 27.5 kcal/mol. The reduced isotopic partition function in **8** is not unusual and the predicted kinetic isotope effect for electron-transfer mediated formation of **8** from **2** is only 1.24. (This assumes that there would still be no barrier from O−O cleavage in

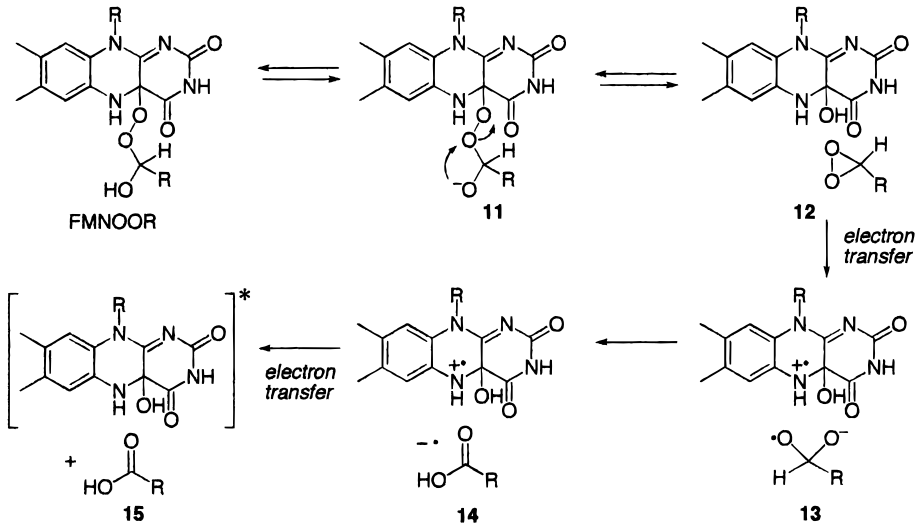

FIGURE 9: A mechanistic proposal for luciferase luminescense, adapted from ref 33.

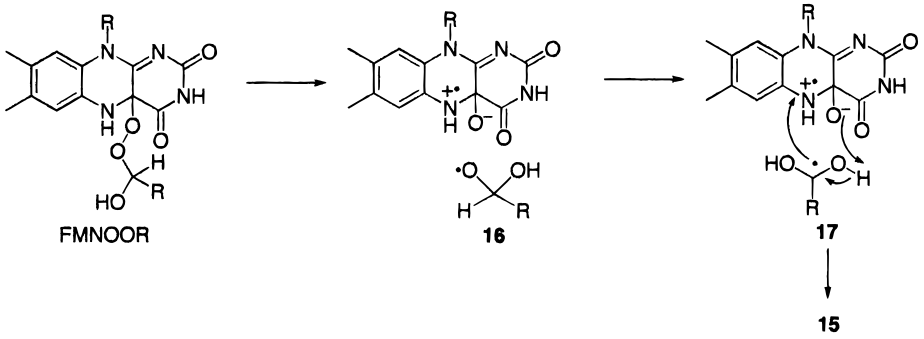

FIGURE 10: The mechanistic proposal of Eckstein et al. (*32*) for luciferase bioluminescense.

the radical anion of **2**.) Thus, the mechanism of Figure 10 does not account for the observed isotope effect. However, either a similar electron-transfer-mediated cleavage of the O−O bond in **11** or a direct formation of **13** from FMNOOR would be predicted to exhibit an isotope effect identical with that of the Figure 9 mechanism, without the intermediacy of a dioxirane. Neither mechanism can be rigorously excluded, though the former would involve an unlikely intramolecular electron transfer to an already negatively charged part of **11**, and the latter would require that both the O−O cleavage in FMNOOR and a proton transfer occur simultaneously with electron transfer and without a barrier to the bonding changes.

It would be difficult to predict from qualitative considerations the isotope effects expected for rate-limiting 1,2-hydrogen rearrangements of **4** or **8** via transition states **5** or **9**, respectively, though such nonlinear hydrogen transfers are sometimes associated with low primary deuterium isotope effects. The ab initio predicted isotope effects for these rearrangements are 4.8 and 4.9, much higher than the experimental value. The inclusion of a correction for tunneling effects [not taken into account in these predictions based on conventional transition state theory (*28*)] would generally increase the predicted isotope effects for these primary hydrogen transfers. Rate-limiting rearrangement of **4** or **8** would therefore not account for the observed isotope effects.

The theoretical calculations support the energetic plausibility of the intermediacy of a dioxirane, and give insight into why a back electron transfer would favor formation of the excited state of the dihydroflavin for this CIEEL (chemically induced electron exchange luminescence) mechanism (*39*). The energy available for back electron transfer to the flavin C4a-hydroxide would be equal to the strain energy in the dioxirane compared to the carboxylic acid (90.0 kcal/mol based on **3** versus **7**), minus the exothermicity of the 1,2-rearrangement (24.6 kcal/mol based on **4** versus **6**), plus the endothermicity of the initial electron transfer. This gives at least 65.4 kcal/mol for the back electron transfer, compared to an energy of 58.4 kcal/mol for the excited state of the FMNOH, based on emission at 490 nm. The modestly exothermic back electron transfer to form the excited-state FMNOH would be expected to occur much faster than electron transfer to form the ground state FMNOH, because the latter would be highly exothermic and well into the Marcus inverted region.

Summary. We have utilized deuterium isotope effects under a variety of reaction conditions to probe the molecular details of the bacterial luciferase catalyzed reaction. Upon the basis of the constancy of the observed isotope effects obtained under a variety of reaction conditions, we have concluded that the isotope effects arise from a single rate-limiting step. Theoretical calculations indicate that the mechanism in Figure 9 involving rate-limiting electron transfer to an intermediate dioxirane is consistent with the unusual aldehydic isotope effect, and that the intermediacy of a dioxirane is energetically plausible. It should be stressed that the existence of the dioxirane intermediate and the radical pair has not been observed directly. However, Kazakov et al. have recently observed the emission of visible light during

the decomposition of dimethyl dioxirane in the presence of aromatic hydrocarbons (*40*). Experiments to spectroscopically detect these proposed intermediates are currently in progress.

ACKNOWLEDGMENT

We thank Dr. Ravindra Topgi for the synthesis of the modified flavins.

SUPPORTING INFORMATION AVAILABLE

Structural drawings, geometries, and energies of structures 1−10 (11 pages). See any current masthead page for ordering information.

REFERENCES

1. Vervoort, J., Muller, F., Lee, J., van den Berg, W. A. M., and Moonen, C. T. W. (1986) *Biochemistry 25*, 8062−8067.
2. Hastings, J. W., Balny, C., Le Peuch, C., and Douzou, P. (1973) *Proc. Natl. Acad. Sci. U.S.A. 70*, 3468−3472.
3. Hastings, J. W., and Balny, C. (1975) *J. Biol. Chem. 250*, 7288−7293.
4. Macheroux, P., Ghisla, S., and Hastings, J. W. (1993) *Biochemistry 32*, 14183−14186.
5. Kurfurst, M., Macheroux, P., Ghisla, S., and Hastings, J. W. (1987) *Biochim. Biophys. Acta 924*, 104−110.
6. Cleland W. W. (1990) in *The Enzymes* (Sigman D. S., and Boyer, P. D., Eds.) 3rd ed., Vol. XIX, pp 99−155, Academic Press, Inc. New York.
7. Presswood, R. P., Shannon, P., Spencer, R., Walsh, C., Becvar, J. E., Tu, S.-C., and Hastings, J. W. (1980) in *Flavins and Flavoproteins* (Yagi, K., and Yamano, T., Eds.) pp 155−160, Japan Scientific Societies Press, Tokyo.
8. Shannon, R. P., Presswood, R. B., Spencer, R., Becvar, J. E., Hastings, J. W., and Walsh, C. (1978) in *Mechanisms of Oxidizing Enzymes* (Singer, T. P., and Ondarza, R. N., Eds.) pp 69−78, Elsevier, North Holland, Amsterdam.
9. Tu, S.-C., Wang, L.-H., and Yu, Y. (1987) in *Flavins and Flavoproteins* (Edmondson, D. E., and McCormick, D. B., Eds.) pp 539−548, Walter de Gruyter, New York.
10. Abu-Soud, H., Mullins, L. S, Baldwin, T. O., and Raushel, F. M. (1992) *Biochemistry 31*, 3807−3813.
11. Abu-Soud, H. M., Clark, A. C., Francisco, W. A., Baldwin, T. O., and Raushel, F. M. (1993) *J. Biol. Chem. 268*, 7699−7706.
12. Degani, I., Fochi, R., and Regondi, V. (1981) *Synthesis 39*, 51−53.
13. Seebach, D., Erickson, B. W., and Singh, G. (1966) *J. Org. Chem. 31*, 4303−4304.
14. Seebach, D., and Corey, E. J. (1975) *J. Org. Chem. 40*, 231−237.
15. Baldwin, T. O., Chen, L. H., Chlumsky, L. J., Devine, J. H., and Ziegler, M. M. (1989) *J. Biolumin. Chemilumin. 4*, 40−48.
16. Kunkel, T. A., Roberts, J. D., and Zakour, R. A. (1987) *Methods Enzymol. 154*, 367−382.
17. Sanger, F. Nickler S., and Coulson, A. R. (1977) *Proc. Natl. Acad. Sci. U.S.A. 74*, 5463−5467.
18. Sinclair, J. F., Waddle, J. J., Waddill, E. F., and Baldwin, T. O. (1993) *Biochemistry 32*, 5036−5044.
19. Whitby, L. G. (1953) *Biochem J. 54*, 437−442.
20. Fritz, B. J., Kasai, S., and Matsui, K. (1987) *Photochem. Photobiol. 45*, 113−117.
21. Williams, C. H., Jr., Arscott, L. D., Matthews, R. G., Thorpe, C., and Wilkinson, K. D. (1979) *Methods Enzymol. 62*, 185−198.
22. Barshop, B. A., Wrenn, R. F., and Frieden, C. (1983) *Anal. Biochem. 130*, 134−145.
23. Zimmerle, C. T., and Frieden, C. (1989) *Biochem. J. 258*, 381−387.
24. Deetz, J. S., Luehr, C. A., and Vallee, B. L. (1984) *Biochemistry 23*, 6822−6828.
25. Hastings, J. W., Baldwin, T. O., and Nicoli, M. Z. (1978) *Methods Enzymol. 57*, 135−152.
26. Nicoli, M. Z., Meighen, E. A., and hastings J. W. (1974) *J. Biol. Chem. 249*, 2385−2392.
27. Frisch, M. J., Trucks, G. W., Schlegel, H. B., Gill, P. M. W., Johnson, B. G., Robb, M. A., Cheeseman, J. R., Keith, T. A., Peterson, G. A., Montgomery, J. A., Raghavachari, K., Al-Laham, M. A., Zakrzewski, V. G., Oriz, J. V., Foresman, J. B., Cioslowski, J., Stefanov, B. B., Nanayakkara, A., Challacombe, M., Peng, C. Y., Ayala, P. Y., Chen, W., Wong, M. W., Andres, J. L., Replogle, E. S., Gomperts, R., Martin, R. L., Fox, D. J., Binkley, J. S., Defrees, D. J., Baker, J., Stewart, J. P., Head-Gordon, M., Gonzalez, C., and Pople, J. A. (1995) Revision A.1, Gaussian, Inc., Pittsburgh, PA.
28. Bigeleisen, J., and Mayer, M. G. (1947) *J. Chem. Phys. 15*, 261.
29. Houk, K. N., Gustafson, S. M., and Black, K. A. (1992) *J. Am. Chem. Soc. 114*, 8565−8572.
30. Beno, B. R., Houk, K. N., and Singleton, D. A. (1996) *J. Am. Chem. Soc. 118*, 9984−9987.
31. Saunders: M., Laidig, K. E., and Wolfsberg, M. (1989) *J. Am. Chem. Soc. 111*, 8989−8994.
32. Eckstein, J. W., Hastings, J. W., and Ghisla, S. (1993) *Biochemistry 32*, 404−410.
33. Raushel, F. M., and Baldwin, T. O. (1989) *Biochem. Biophys. Res. Commun. 164*, 1137−42.
34. Cho, K.-W., and Lee, H.-J. (1984) *Korean J. Biochem. 17*, 1−9.
35. Kirsch, J. F. (1977) in *Isotope Effects on Enzyme Catalyzed Reactions* (Cleland, W. W., O'Leary, M. H., and Northrop, D. B. Eds.) pp 100−121, University Press: Baltimore, MD.
36. Eberhard, A., and Hastings, J. W. (1972) *Biochem. Biophys. Res. Commun. 47*, 348−353.
37. Ahrens, M., Macheroux, P., Eberhard, A., Ghisla, S., Branchaud, B., and Hastings, J. W. (1991) *Photochem. Photobiol. 54*, 295−299.
38. Gould, I. R., and Farid, S. (1988) *J. Am. Chem. Soc. 110*, 7883.
39. Schuster, G. B. (1979) *Acc. Chem. Res. 12*, 366−373.
40. Kazakov, D. V., Kabalnova, N. N.; Voloshin, A. I., Skereshovets, V. V., and Kazakov, V. P. (1995) *Russ. Chem. Bull. 44*, 2193−2194.

BI972266X